# 3D-Printed Biomimetic Super-Hydrophobic Structure for Microdroplet Manipulation and Oil/Water Separation

*Yang Yang, Xiangjia Li, Xuan Zheng, Zeyu Chen, Qifa Zhou, and Yong Chen**

**Biomimetic functional surfaces are attracting increasing attention for various technological applications, especially the superhydrophobic surfaces inspired by plant leaves. However, the replication of the complex hierarchical microstructures is limited by the traditional fabrication techniques. In this paper, superhydrophobic micro-scale artificial hairs with eggbeater heads inspired by *Salvinia molesta* leaf was fabricated by the Immersed surface accumulation three dimensional (3D) printing process. Multi-walled carbon nanotubes were added to the photocurable resins to enhance the surface roughness and mechanical strength of the microstructures. The 3D printed eggbeater surface reveals interesting properties in terms of superhydrophobilicity and petal effect. The results show that a hydrophilic material can macroscopically behave as hydrophobic if a surface has proper microstructured features. The controllable adhesive force (from 23 µN to 55 µN) can be easily tuned with different number of eggbeater arms for potential applications such as micro hand for droplet manipulation. Furthermore, a new energy-efficient oil/water separation solution based on our biomimetic structures was demonstrated. The results show that the 3D-printed eggbeater structure could have numerous applications, including water droplet manipulation, 3D cell culture, micro reactor, oil spill clean-up, and oil/water separation.**

Nature provides a wide range of functional surfaces, which inspires the study of biomimetic smart surface for various practical applications.[1–4] One of the interesting inspiration is the super-hydrophobic surfaces, which have attracted great attention because of the high scientific and economic interests, such as self-cleaning, antisticky, oil/water separation, microreactors, and microdroplet manipulation.[5–15] One classical example is the super-hydrophobic surface with lotus effect for self-cleaning. Water droplet forms almost perfect sphere and slides easily on the hierarchically structured lotus leaf consisting of nanostructure hydrophobic wax crystals.[16] Another example is the unique combination of hydrophilic path on super-hydrophobic surfaces ("Salvinia effect"), which demonstrates an effective design for long-term air retention and droplet manipulation.[17,18] The hierarchical architecture of the leaf surface is dominated by complex elastic eggbeater-shaped hairs coated with nanoscopic wax crystals and hydrophilic patches on the terminal cells. Many efforts have been performed to produce artificial biomimetic super-hydrophobic surfaces. For example, the super-hydrophobic films prepared by electro-deposition and hydrothermal methods with mesh-like, ball cactus-like, and tilted nanorod structures.[19–21] However, some of the complicated architectures in nature far exceed the capability of the traditional fabrication techniques, which hinders the progress of biomimetic surface study. The eggbeater structures with sizes 100 times scale down compared with the real features in nature were fabricated by lithography. However, the contact angle is only 122° (not super-hydrophobic) and the air volume generated on the bottom surface is limited due to the dimension of such microfeatures.[19] High water contact angles with salvinia effect have been obtained by coating carbon nanotube on stainless steel surface.[22] To mimic salvinia effect, additive manufacturing (3D printing) that has wide applications in industry, academia and daily usages could be an effective way to fabricate such complicated architectures.[23,24]

Here we present an innovative way to fabricate biomimetic super-hydrophobic eggbeater structure with controllable surface morphology. The artificial surfaces with interesting structure-related functions were replicated according to the eggbeater structure design in *Salvinia molesta* hairs by using a novel additive manufacturing process named immersed surface accumulation based 3D (ISA-3D) printing. This technique, based on the accumulation of material along the movement of light guide tool inside photocurable resin, allows one to realize the fabrication of multiscale structures on the surface of an inserted object. Furthermore, the

Dr. Y. Yang, X. Li, Prof. Y. Chen
Epstein Department of Industrial and Systems Engineering
University of Southern California
3715 McClintock Ave, Los Angeles, CA 90089-01932, USA
E-mail: yongchen@usc.edu
X. Zheng, Prof. Y. Chen
Department of Aerospace and Mechanical Engineering
Viterbi School of Engineering
University of Southern California
3650 McClintock Ave, Los Angeles, CA 90089, USA
Dr. Z. Chen, Prof. Q. Zhou
Department of Biomedical Engineering
Viterbi School of Engineering
University of Southern California
1042 Downey Way, Los Angeles, CA 90089, USA

**DOI: 10.1002/adma.201704912**

controllable features (size, number of eggbeater arms, gap distance) were tailored to study their effects on the hydrophobic property and water adhesion. In addition, multiwalled carbon nanotubes (MWCNTs) were added in liquid resin because of their ability to remove the static charges accumulated on the surfaces and to increase surface roughness.[25,26] The unusual wetting characteristics of an eggbeater surface are governed by both chemical composition and geometric structure.[7,27]

The 3D printed surfaces show super-hydrophobicity and structure-dependent water adhesion. The adhesive force is easily tuned (23–55 μN) with the increment of number of eggbeater arms, which is different from other fabrication methods such as by controlling the density and diameter of nanotubes.[14,21] This special capability allows nonloss water transportation for applications such as the droplet-based microreactors. The petal effect of the eggbeater surface makes it suitable for 3D cell culture to naturally mimic avascular tumor with inherent metabolic and proliferative gradients.[28] The advantages of this technique enable its potential use as a new low cost toolbox for 3D culture in cell or tissue engineering. Besides, oil/water separation has been a worldwide subject because of the increasing release of industrial oily waste water as well as frequent crude oil leakage.[29] Here we demonstrate that our 3D-printed eggbeater structure presents an effective way of oil absorption and oil/water separation attributed to the different interfacial effects of oil and water for future separation device design.

Plant and animal species that survive on the water surface have evolved special super-hydrophobic air-retaining properties to prevent wetting and submersion. In the "lotus effect," the water droplet has a large contact angle (CA ≈161°) and a low sliding angle (2°) on the surface.[30] In contrast, for the "petal effect," the Rose petals show super-hydrophobicity (CA ≈ 152°) with strong adhesion that pins water droplets.[31] Inspired by these plants, artificial super-hydrophobic surfaces have attracted much interest due to their potential applications, e.g., in self-cleaning, oil/water separation, antireflection, and microdroplet transportation.[5–15,32] In these applications, controlling the liquid adhesion toward the target surface is particularly important because it is the adhesive property that ultimately determines the dynamic action of the liquid on the surface.[33]

The upper side of the floating leaves of *S. Molesta* is densely covered with complex multicellular hairs (**Figure 1**a) to form a super-hydrophobic surface (Figure 1b). The terminal ends of the four hairs are connected, forming an eggbeater-shaped structure (Figure 1c). Recent research shows that even a hydrophilic material can macroscopically behave as hydrophobic if surface has certain microstructured features.[19,34] Inspired

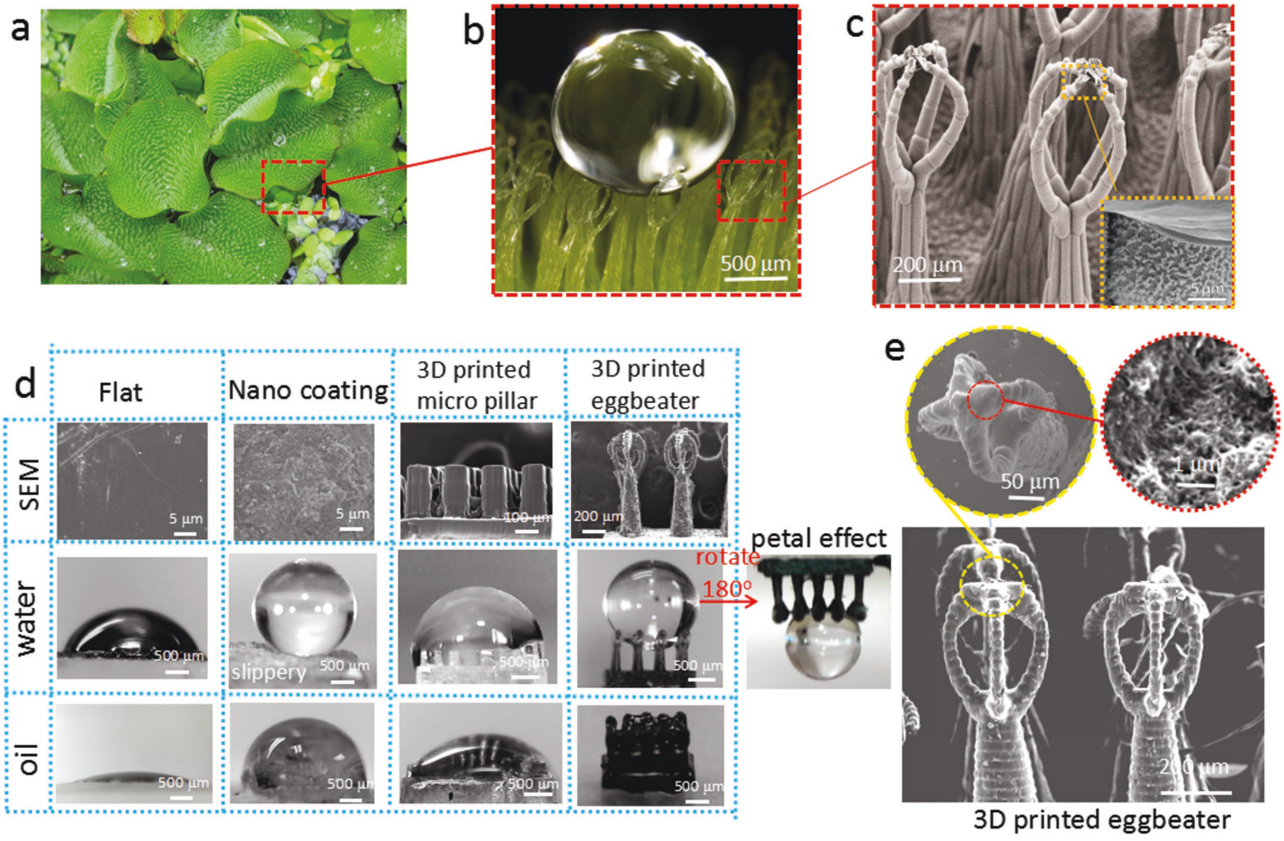


**Figure 1.** Biomimetic super-hydrophobic structure. a) Morphology of *S. Molesta* leaf, upper side of the leaf surface is densely covered with eggbeater hairs; b) a spherical water droplet on top; c) SEM image of the eggbeater hair structure, (a–c) reproduced with permission.[59] Copyright 2016, IOP Publishing; d) water and oil on the flat surface, after nanocoating, 3D printed micro pillar surface and 3D printed eggbeater surface; e) SEM images of 3D-printed eggbeater arrays (the insert image shows the magnification of one hair).

by this work, microscale super-hydrophobic eggbeater structures were designed and fabricated based on a hydrophilic photocurable resin by 3D printing (see the Experimental Section). The flat surface made with E-glass/MWCNT shows hydrophilic and super-olephilic properties. After sputtering nanoscopic coatings on the surface, the flat surface shows super-hydrophobic (slippery surface) and olephobic property (Figure 1d). For the 3D-printed pillar arrays, the structure shows hydrophobic and olephilic property. A series of hierarchical structures with eggbeater hairs on the top of pillar arrays were fabricated by the developed ISA-3D printing process to mimic the *S. Molesta* leaf. The stalk of an artificial hair has a height of 700 μm and a diameter of 300 and 150 μm on the bottom and top, respectively. The head is fabricated by intersecting different number of circumferences with a diameter of 35 μm and a height of 250 μm (Figure 1e). The sizes are designed according to the eggbeater and pillars in nature. The results show the 3D-printed eggbeater surface has a strong hydrophobicity and a good controllability of water droplet by turning upside down (Petal effect) as well as super-olephilic property (Figure 1d). The petal effect is attributed to the high adhesion of hydrophilic tips (discussed below). Besides, the contact angle hysteresis is tested to be 69.5° for the 3D printed eggbeater structure. A comparison of our work with others is shown in **Table 1**. The super-hydrophobic property of our 3D-printed structure is attributed to the surface tension and the low surface fraction of the contact area between the water droplet and the eggbeater tip. The four arms bent together at the terminal ends to create as much surface per height difference as possible to maximum the energy that is required for the water to penetrate into the region. The simulation by Comsol MultiPhysics (Figure S5, Supporting information) shows that the elastic properties of the eggbeater hairs allow a small deformation of the air–water interface in both directions to restore the equilibrium position. The Salvinia effect opens intriguing perspectives for designing artificial surfaces on the basis of the super-hydrophobic and super-olephilic properties for a wide range of applications such as droplet control, nonloss microdroplet transport, drag reducing surface coating, and oil/water separation.

Inspired by the computer numerically controlled (CNC) accumulation process,[38–40] an immersed surface accumulation based 3D printing process has been developed (**Figure 2**a). The key component of the ISA-3D printing system is a light guide tool consisted of optical fibers and objective lens for continuous 2D light beam projection (Figure S1, Supporting Information). The light guide tool is merged inside a tank that is filled with photocurable liquid resin (E-glass/MWCNTs) (Figure 2b). Combining both dynamically controlled light beam projection with the 5-axis movement of the light guide tool, the ISA-3D printing method can construct microscale features on the surface of a macroscale object by selectively curing liquid resin into solid. Unlike most additive manufacturing processes, the ISA-3D printing can be applied to modify the surface functionality of an inserted object (Figure 2e). For the surface accumulation process, a straight light guide tool (light intensity 28.5 mW $cm^{-2}$) is merged inside liquid photocurable resin. To generate high resolution 2D patterned light beam, a digital micromirror device (DMD) chip is applied in the optical imaging system (Figure 2b). Accordingly, the resin is solidified by the 2D patterned light beam defined by the DMD chip on the top surface of the light guide tool. After the first cured layer is attached on the inserted object, the guide tool moves away with a designed speed. During the movement, sufficient resin will fill the curing area since the light guide tool is immersed in liquid resin. The cured resin can be safely detached from the light guide tool by applying a polydimethylsiloxane coating on the tip of the optical fiber (Figure 2e). The dimension of the light beam used in our prototyping system for resin accumulation is 3.67 mm × 2.75 mm. Since the resolution of the DMD chip is 1920 × 1080, the resolution of the light beam in our ISA-3D printing system is 2.5 μm per pixel. In addition, the relative position of the light guide tool and the preexisting object can be determined using the integrated vision system. In the further study, other light guide tools in different shapes and sizes will be designed to address the problem of building features on object surfaces with different orientations.[41]

**Table 1.** Comparison of the 3D-printed super-hydrophobic structure with other works.

| Method | Contact angle | Super-hydrophobic | Scale (compared with nature) | Adhesive force | Nonloss transport | Oil/water separation | Ref. |
|---|---|---|---|---|---|---|---|
| Natural plant (*S. Molesta*) | 152° | √ | Multiscale | Uncontrollable | × | √ | [17] |
| Electrospinning | 166.5° | √ | Nanoscale | Uncontrollable | × | × | [9] |
| Membrane template | 162° | √ | Nanoscale | Controllable | √ | × | [14] |
| Electrochemical anodizing | 152–160° | √ | Nanoscale | Controllable | × | × | [21] |
| Membrane template | 160° | √ | Nanoscale | Uncontrollable | √ (magnetic field) | × | [33] |
| Vapor corrosion, Thiolate reaction | 155–160° | √ | Nanoscale | Controllable | √ | × | [35] |
| Dipcoating | 150–155° | √ | 2 μm | Controllable | √ | × | [36] |
| Ink-jet printing | 155–160° | √ | Micro: 20 μm | Uncontrollable | × | √ | [37] |
| Lithography | 122° | × | 100 times scale down (micro) | Uncontrollable | × | × | [19] |
| Our ISA-3D Printing | 152–170° | √ | 1:1 to Nature, multiscale (micro–mesoscale) | Controllable | √ | √ | Our work |

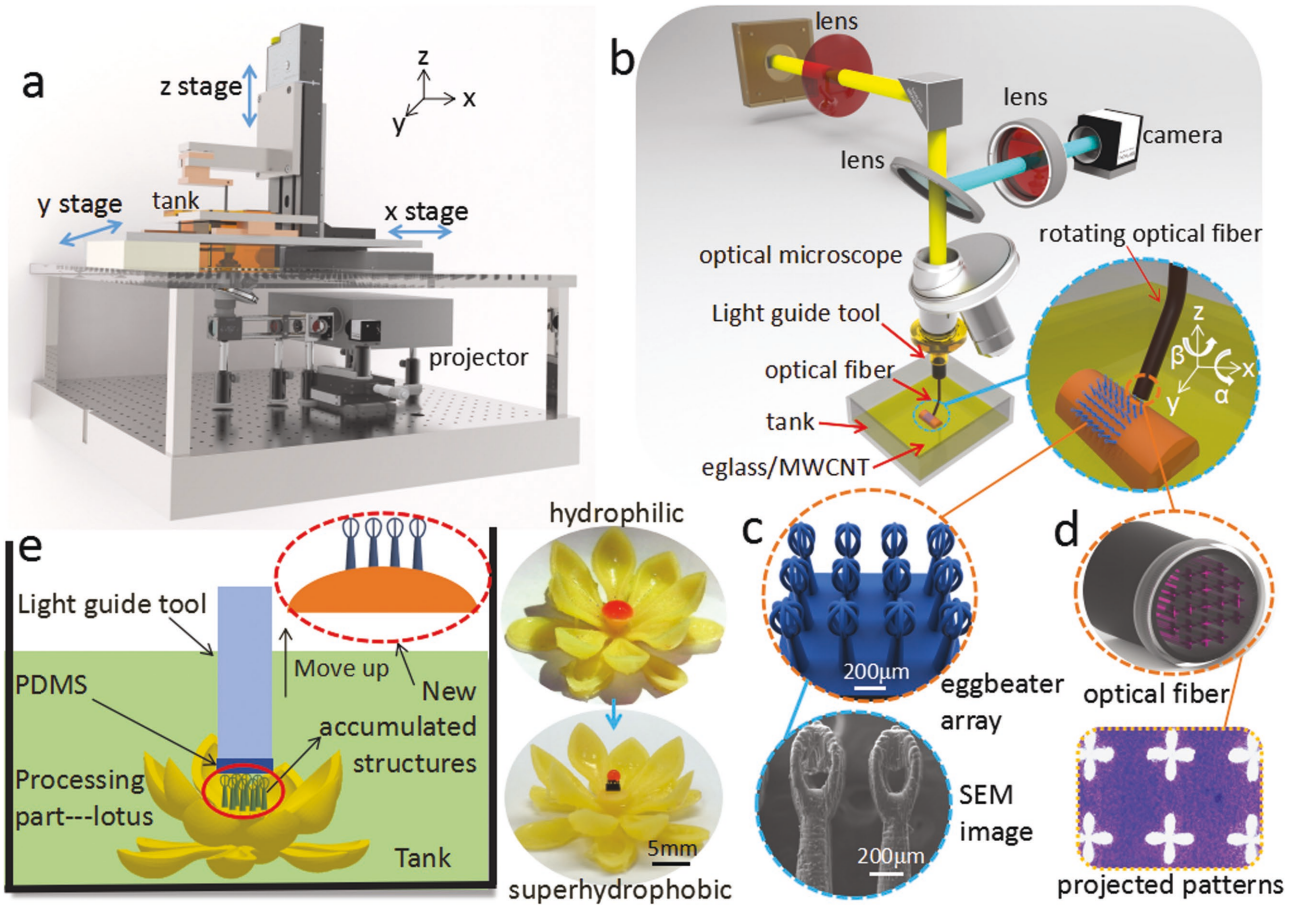


**Figure 2.** a) Schematic diagram of the immersed surface accumulation based 3D printing (ISA-3D) process; b) the optical system in the ISA-3D printing process (insert shows the magnification of light guide tool and optical fiber in (d) with projected 2D micro patterns); c) models and SEM image of the 3D-printed eggbeater arrays; and e) an illustration of adding microscale eggbeater structure on the free form curve surface of a lotus flower model, which changes the surface from hydrophilic to super-hydrophobic by using a straight light guide tool.

The biomimetic micro eggbeater structure is designed by Solidworks and fabricated using the ISA-3D printing process. **Figure 3**a shows the 3D-printing process of the structure by using E-glass/MWCNTs composites. The process planning setting for the ISA-3D printing process (Figure S1k,l, Supporting Information) is discussed in the Experimental Section. The arrays of artificial hairs used in the tests were arranged by following a 2D hexagonal lattice structure with spaces $d = 400$ μm between neighbor stalks. As shown in Figure 3 b–e, designs with different number of eggbeater arms were fabricated to study its effect on the super-hydrophobic property of the bioinspired structure. The excellent mechanical property of carbon nanotubes makes the 3D-printed hairs stable. Hence the suspended eggbeater structure will not collapse nor adhere with each other (the modulus was increased from 161 to 455 MPa with 0.5 wt% MWCNT). Besides, the super-hydrophobility increases with the addition of MWCNTs because of the increment of surface roughness (Figure S4, Supporting Information). Eggbeater structures were fabricated in the form of square array with lateral size 3.67 mm × 2.75 mm (4 × 5 array). The results show that the 3D-printed eggbeater structure behaves as a super-hydrophobic surface, even though the component material (E-glass with MWCNT) shows hydrophilic behavior on flat configuration (a contact angle of 65° on flat surface) (Figure 3f). The super-hydrophobic properties were studied by adjusting the number of eggbeater arms and the gap distance between each stalk of the artificial hair (Figure 3f). The artificial surface proved to be super-hydrophobic with a contact angle of 170° for $N = 2$, $d = 0.5$ mm and 152° for $N = 4$, $d = 0.4$ mm (Figure 3g) (Figure S3, Supporting Information). It is noticed that the printed structure with $N = 0$ possess a Wenzel state where the water droplets are pinned in the pillar arrays (Figure 3f). Hence the enhancement of super-hydrophobic property is attributed to the eggbeater structure on the surface.

For $N \geq 2$, due to the hydrophilic property of the composite that we used, the water droplet is partially merged inside the eggbeater arms but not through the whole structure to the bottom. In this case, air is trapped between different eggbeater arrays.[17,19,42] As reported, there are four different kinds of contact regime for the eggbeater structure in contact with water W–W, CB–CB, $W_M$–$CB_m$, $CB_M$–$W_m$ (W represent Wenzel; CB represents Cassie–Baxter; subscript "M" is for "Macro," "m" is for "micro").[19] For the CB–CB state, the contact angle is predicated by

$$\cos\left(\theta_{CB}^{CB}\right) = f_{SL}\cos(\theta) - f_{LA} \quad (1)$$

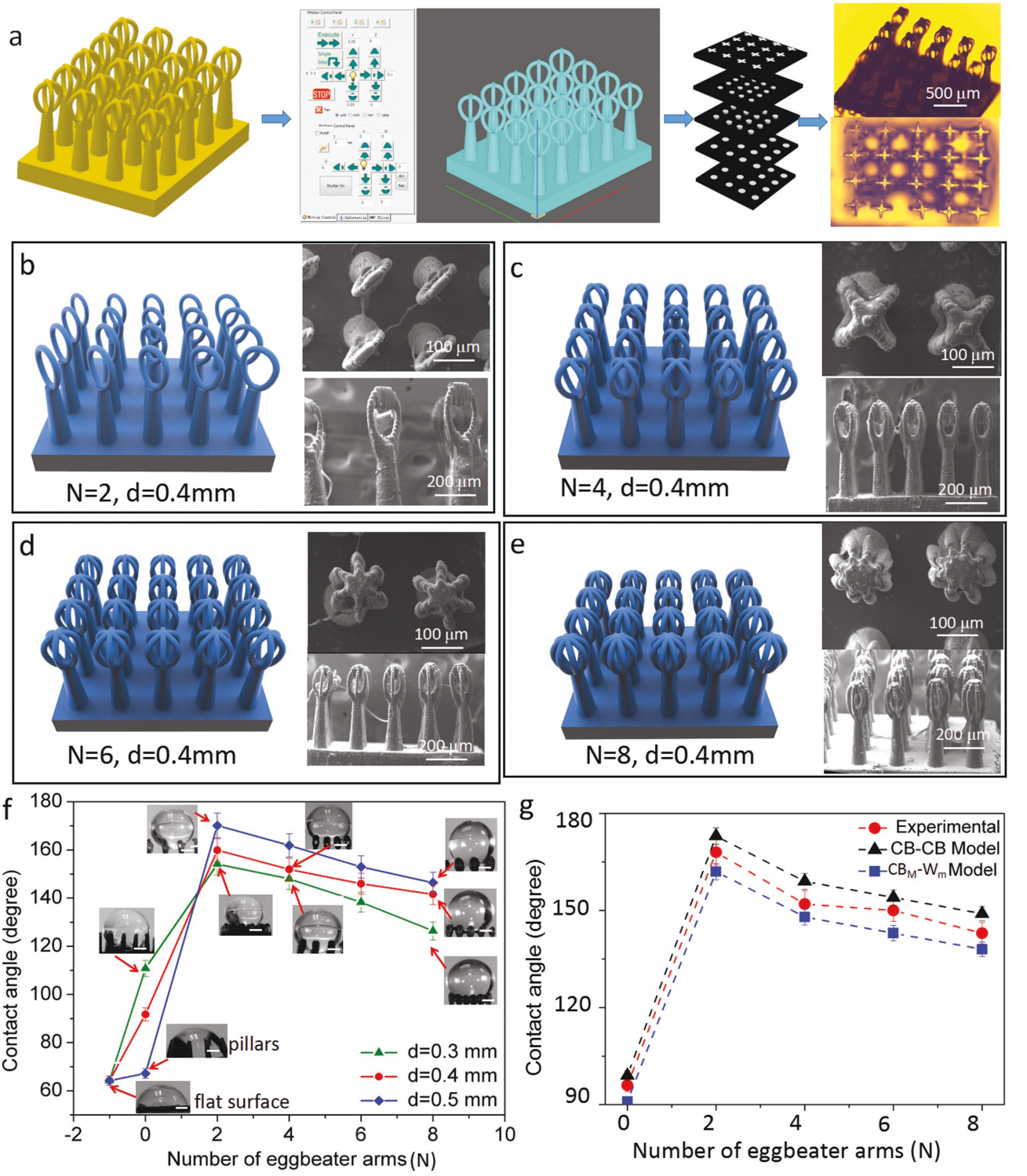


**Figure 3.** Schematic diagram of the fabrication process of eggbeater structures by the ISA-3D printing. a) The eggbeater array model by Solidworks, sliced in our digital micromirror device based Stereolithography (DMD-based SL) software and optical microscopy images show the side and top views of the printed parts; the models and SEM images of the 3D-printed eggbeater arrays with different number of arms (b, $N = 2$; c, $N = 4$; d, $N = 6$; e, $N = 8$); f) contact angle and test pictures for different numbers of $N$ and gap distance $d$ (scale bar 500 μm); and g) a comparison of the experimental and simulated contact angles with CB–CB and W–CB models for different patterns.

Here $f_{SL}$ and $f_{LA}$ represent the fraction of solid–liquid interface and liquid–air interface, respectively.[19] As for the mixed $CB_M$–$W_m$ state (lower/macro-Cassie–Baxter and upper/micro-Wenzel) with the water droplet pinned on the top of eggbeater arms and an air layer is trapped between the substrate and the bottom of hairs' heads. The contact angle can be predicted by

$$\cos\left(\theta_{CB}^{W}\right) = Rf_{SL}\cos(\theta) - f_{LA} \quad (2)$$

Interestingly Equation (2) predicts a hydrophobic behavior of the structured surface ($\theta_{CB}^{W} > 90°$) even if $\theta < 90°$ (i.e., pristine hydrophilic material), if the following condition is satisfied $F_{LA} \geq R\cos(\theta)/[1 + \cos(\theta)]$ $F_{LA} \geq R\cos(\theta)/[1 + \cos(\theta)]$.[19] It is noticed that the surface roughness of the eggbeater structure is increased with the addition of MWCNT (Figure S3b, Supporting Information), which increases the super-hydrophobicity. The predicated $\theta_{CB}^{CB}$ and $\theta_{CB}^{W}$ is 154° and 149°, respectively. The test results of our 3D-printed structures (152°) are between these two states (Figures S3b and Figure S4, Supporting Information). Together with the optical microscope images, we believe the presence of a $CB_M$–$W_m$ regime in the middle and CB–CB regime in the edges when the 3D printed surface is in contact with water droplet. This CB regime in the edges provides enough liquid air contact area to support the super-hydrophobic effect, and the micro-Wenzel ($W_m$) state in the middle makes the high CA hysteresis and petal effect.

The contact angle decreases with the increment of *N*. This is attributed to the increase of contact area between the eggbeater tip and the water droplet. However, the eggbeater structure with two arms ($N = 2$) is fragile and easy to break during our test (the simulation results support the test, which show the largest deformation exists in the eggbeater arrays with $N = 2$ and the smallest for $N = 8$. This is because less stress is distributed on each arm with the increment of *N* (Figure S5, Supporting Information). Therefore, the best performance of the eggbeater arrays is $N = 4$ if considering both super-hydrophobicity and strength of the structure. Besides, the hydrophilic tip of the eggbeater arrays is causing zero velocity conditions at the surface of the wetted area. This will promote the stabilization of the air–water interface at a predefined level on top of the hairs.[17] The arms are bent together at the terminal ends to create a minimization of the contact area. The energy required for the water to penetrate into the region between the hairs is maximized in order to stabilize the air–water interface efficiently. Therefore, the hairs are split into four arms to create as much surface per height difference as possible. The elastic properties of the eggbeater hairs are advantageous to prevent the rupture of the contact of air–water interface. The simulation results by Comsol Multiphysics demonstrate that there are deformations at the air–water interface when the water droplet is on top of the arrays (Figure S5, Supporting Information). The elastic mechanical forces of the deformed hairs described by Hooker's law can help to restore the equilibrium position of the water droplet on the top of eggbeater arrays.

Surface outgrowths such as hairs or trichomes widely occur on biological surfaces. They sometimes have unique adhesive and elastic properties that are optimally adapted to specific functional requirements. The adhesive force of the 3D-printed eggbeater structures plays a key role in understanding the biomimetic structures. Here the adhesive force of the 3D-printed tips was investigated to better understand the petal effect for water droplet manipulation. A method of capillary adhesion technique was used to evaluate the tip adhesive force for different numbers of *N*. It involves the creation and development of a liquid meniscus upon touching a liquid surface with the structure, and the subsequent disruption of this liquid meniscus upon removal.[43] The evaluation of the meniscus shape immediately before snap-off allows the quantitative determination of the liquid adhesive force. In our study, a meniscus from a flat water surface until rupture occurs in order to determine the adhesive force.

The force pulling at the trichome tip is equal to its water adhesion force, which is given by $F = \frac{\partial W}{\partial b} = \frac{\partial A}{\partial b} \cdot \sigma$ (see the Experimental Section and Figure S6, S7, Supporting Information). The comparison shows the adhesive force increases with the number of *N* (Figure S7, Supporting Information). It is noticed that the average tip adhesive force of the 3D-printed eggbeater structure is $F = 29.3$ μN (for $N = 4$), much larger than the eggbeater-shaped trichome on the *S. Molesta* leaves ($F = 19.5$ μN).[43] For the 3D-printed array, the adhesive force is calculated to be $\approx 4 \times 5 \times 29.3 = 586$ μN, which is much larger than the gravity force of one droplet ($3\ \text{mg} \times 9.8\text{N kg}^{-1} \approx 29.4\ \mu\text{N}$). It demonstrates that the large water adhesive force presenting at the tips of the eggbeater structures is a key factor for the petal effect. Like the *S. Molesta* leaves, this large water adhesion force of the 3D-printed eggbeater-shaped hairs is also one key factor for the persistence of the air layer on the surface due to the pinning of the air–water interface.[17]

The controllable adhesion allows the obtained super-hydrophobic eggbeater microstructures to be used for a wide variety of applications. Liquid droplets are usually transported by utilizing another immiscible liquid as a flow carrier, which is proven to be rather cumbersome since a large quantity of reagent is consumed.[44] On the contrary, the manipulation of microdroplets in a drop-to-drop setting is a simple and efficient way for the liquid droplet based microreactor systems due to its advantages of high flexibility and low cost.[45] Herein, we demonstrate an application of the 3D-printed eggbeater structure with high adhesion in the liquid-droplet-based microreactors. In the test, syringe needles were used to transport different types of water droplets and our 3D-printed super-hydrophobic structures were used as the reaction substrate. A water droplet (2 μL) containing $FeCl_3$ (0.5 mol $L^{-1}$) was first deposited onto the super-hydrophobic surface (**Figure 4**a) and then another droplet containing KOH (3 mol $L^{-1}$) was added. The two droplets coalesced after contact and brown $Fe(OH)_3$ was produced due to the reaction between $Fe^{3+}$ and $OH^-$ (Figure 4a): $FeCl_3 + 3KOH = Fe(OH)_3\downarrow + 3KCl$. The droplet keeps a round shape due to the super-hydrophobic property of the eggbeater surface. The comparison shows that the products of $Fe(OH)_3$ turn from dark brown to light brown with the decrease of mole ratio of KOH from 1.5 to 0.3 mol $L^{-1}$ (Figure 4 b,c). The phenomenon is easy to observe with the microscope due to the super-hydrophobic structures and the mixed droplets staying on the surface for a long time. This method based on microdroplet retention has the advantages of high flexibility, significant

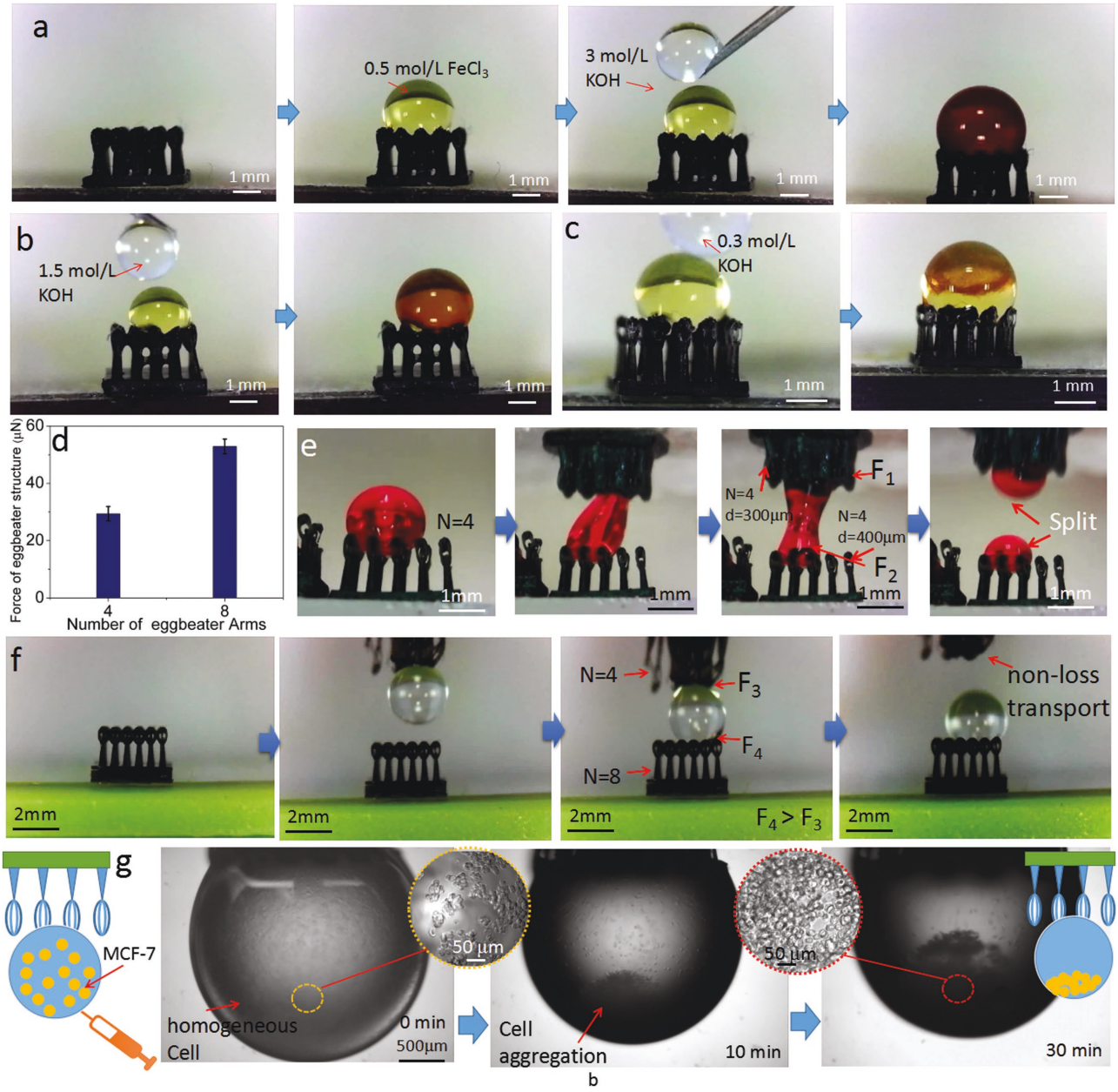


**Figure 4.** Demonstration of some applications of the 3D-printed super-hydrophobic eggbeater structure a) A water droplet based microreactor; b,c) the reaction of $FeCl_3$ (0.5 mol $L^{-1}$) with various mole ratios of KOH to generate different colors of products; d) adhesive force of eggbeater structure for $N = 4$ and $N = 8$; e) split process of one dyed water droplet by two eggbeater structures, both with $N = 4$; f) pictures show the nonloss water transport process from an eggbeater structure ($N = 4$) to another one with larger adhesive force ($N = 8$); g) for the 3D Cell Culture, Breast Cancer cell (MCF-7) aggregation process in one droplet hanging on the printed eggbeater structure ($N = 4$), insert figure shows the top view of homogeneous cells and aggregated cells (cell density 50 000 cell $mL^{-1}$), the droplet size change is attributed to the evaporation of nutrition liquids over time.

material saving, and low cost to distinguish different mole ratio of solvents. Such droplet-based microreactor has shown significant advances in protein crystallization, enzymatic kinetics, and other biochemical reactions.[46]

The water adhesive force of eggbeater structure can be adjusted and increases with the increment of eggbeater arms (from 23 μN for $N = 2$ to 55 μN for $N = 8$, Figure 4d and Figure S7, Supporting Information). The tunable effect of the adhesion is ascribed to different wetting states and the changes of contact areas between the eggbeater arms with water droplet. Two eggbeater structures with $N = 4$, $d = 300$ μm and $N = 4$, $d = 400$ μm were used to split the droplet (Figure 4e). The results show that the dyed water droplet was split into two parts that stay on the eggbeater structure. The split process is attributed to the similar adhesive force for $N = 4$, $d = 300$ μm and $N = 4$, $d = 400$ μm ($F_1 \approx F_2$, assuming that the contact areas on the top and bottom are similar). In comparison, the nonloss water droplet transport can be achieved by using the eggbeater

structures with significantly different adhesive forces. As shown in Figure 4f, a water droplet was first placed on the printed eggbeater super-hydrophobic surface with $N = 4$ (step 1). Then the sticky patterned surface was put upside down for the transport (step 2). It was then completely transferred from the surface $N = 4$ to the surface $N = 8$ (step 3) ($F_3 = 469\ \mu N << F_4 = 880\ \mu N$). Finally, the water droplet was released and keeps the round shape on the surface for $N = 8$ (step 4). Hence the 3D-printed eggbeater structure can be used as a microhand to transfer small water droplets (2 µL) from a super-hydrophobic surface to another one without loss or contamination, which may lead to applications such as microsample analysis.[14,47,48]

Using a 3D cell culture technique to grow cells can more closely mimic natural tissues and organs than growing cells in 2D. In 2D cell culture, cells are grown on flat dishes made of polystyrene plastic that is very stiff and unnatural. The cells adhere and spread on this plastic surface and form unnatural cell attachments to proteins that are deposited and denatured on this synthetic surface.[49] In comparison, cells attach to one another and form natural cell-to-cell attachments in 3D cell culture, which is flexible and pliable like natural tissues. Recent studies have confirmed that 3D cultured tumor spheroid is more resistant to drugs compared with 2D cell cultures due to cell–cell contact response and internal protective mechanisms.[50] To make 3D cell culture, our eggbeater structure was tested based on its petal effect. It was found that cell suspension droplets were well fixed on the 3D-printed structure. First the eggbeater structure was put upside down for the addition of droplet containing MCF-7 cancer cells and nutrition. The process was monitored in an optical microscope. The cancer cells show homogeneous distribution in the droplet initially and then aggregate to the bottom to form a spheroid. The cell spheroid was developed by gravity in the suspended droplets, which provides a 3D environment that more accurately recapitulates the in vivo tumor compared to 2D cell culture (Figure 4g). In this 3D cell culture environment, cells can exert forces on one another as well as move and migrate as they do in vivo.

The previous study demonstrates that super-hydrophobic eggbeater structure with controllable adhesion have various potential applications, such as nonloss transport of microdroplets, the analysis of very small volumes of liquid samples, tissue engineering, drug discovery, and drug delivery monitoring.

Environmental protection and economic development have increased the demand for materials that can effectively separate oil–water mixtures.[51–53] The petroleum industry also requires novel oil–water separation methods to improve oil recovery.[54] For the oil/water separation, previous researches are mainly focused on the micro and nanostructures with special wettability including polymer-coated, hydrogel-coated and surface-modified meshes and polymer networks.[10,12,55] The separation of oil/water mixture by membrane with externally applied pressures[56] and electric field-driven methodology for the separation of oil/water mixture are reported.[57,58] However, this methodology requires continuous application of a very high voltage or pressures. Here, inspired by the oil absorption ability by *S. Molesta* leaf,[59] we present an easy way for efficient oil/water separation by using our 3D-printed eggbeater structure.

Our separation methodology is solely using the difference in capillary forces acting on the two phases. It is shown to be fast and highly energy-efficient. Oil droplet quickly merged into the 3D-printed eggbeater structure, demonstrating a super-oleophilic property (Figure S9a, Supporting Information). The super-hydrophobic and super-olephilic property of the printed eggbeater structure is attributed to the higher surface tension of water than oil and the olephilic nature of polymer used.[60] In the methodology of capillary-force-based separation (CFS), the wetting phase permeates through the membrane, whereas the nonwetting phase is retained. For the CFS based system to work effectively, it is necessary that the wetting phase contacts the structure. There are several techniques to achieve this goal: gravity-driven (if the wetting phase has a higher density than the nonwetting phase), electrostatic (if the wetting phase is a polar liquid).[61,62] In this work, we demonstrate that the CFS based eggbeater structure can act well for the oil/water separation at different conditions (flat, tilt for 45° and 90° and even upside down for 180°, **Figure 5** c–e). The wetting phase (oil) will merge into the eggbeater structure and keep the nonwetting phase (water) on the top to form a spheroid shape. This separation method solely utilizes the adhesion of oil (even antigravity) to engender the separation of various oil–water mixtures. The oil/water separation efficiency is tested to be 99.9% by using thermogravimetric analysis (TGA) (Figure S10, Supporting Information)

The efficiency of oil absorption can be referred to as weight gain, i.e., wt%, defined as the weight of absorbed oil per unit weight of dry eggbeater structure. 6 mg dyed oil was absorbed by eggbeater structure (0.5 mg) in 1 s (the absorption is fast and is shown in Video 3 in the Supporting Information), showing an average absorption rate (weight gain per second) of 12 g $g^{-1}$ $s^{-1}$. This value is lower than the carbon aerogel (68 g $g^{-1}$ $s^{-1}$),[63] but is comparable to CNT sponge (6–20 g $g^{-1}$ $s^{-1}$)[64] and much larger than Graphene sponge (0.57 g $g^{-1}$ $s^{-1}$),[65] Cu foams (≈1 g $g^{-1}$ $s^{-1}$),[66] and NPs/PTEE-coated PU sponge (2 g $g^{-1}$ $s^{-1}$).[67] The 3D printed device can quickly and selectively absorb and collect a variety kinds of oils (light and heavy crude oil, corn oil, and vacuum oil) from a polluted water surface (Figure S9, Supporting Information), showing a high absorption capacity and high recycle efficiency after several cycles test. The device can be easily scaled up for large area oil absorption and separation due to its high absorption rate. Our study shows that it facilitates a simple and low cost approach for efficient oil spill cleanup and oil/water separation.

In conclusion, we have demonstrated the fabrication of complex bioinspired eggbeater patterns by the ISA-3D printing process to replicate the morphology of the *S. Molesta* leaves. The artificial eggbeater structure, made with a hydrophilic material, shows remarkable super-hydrophobic property and petal effect. The super-hydrophobic property and tunable adhesion is related to the number of eggbeater arms and the gap distance between each hair. It opens intriguing perspectives for designing artificial surfaces on the basis of eggbeater structure to form a super-hydrophobic surface. Based on the study, we demonstrated the potential applications in the droplet-based microreactors, nonloss water transport, 3D cell culture and oil/water separation via our 3D-printed eggbeater structures. We believe that the reported results would be helpful to further understand the effect of wetting states on the surface adhesion and the fabrication principle for a super-hydrophobic surface

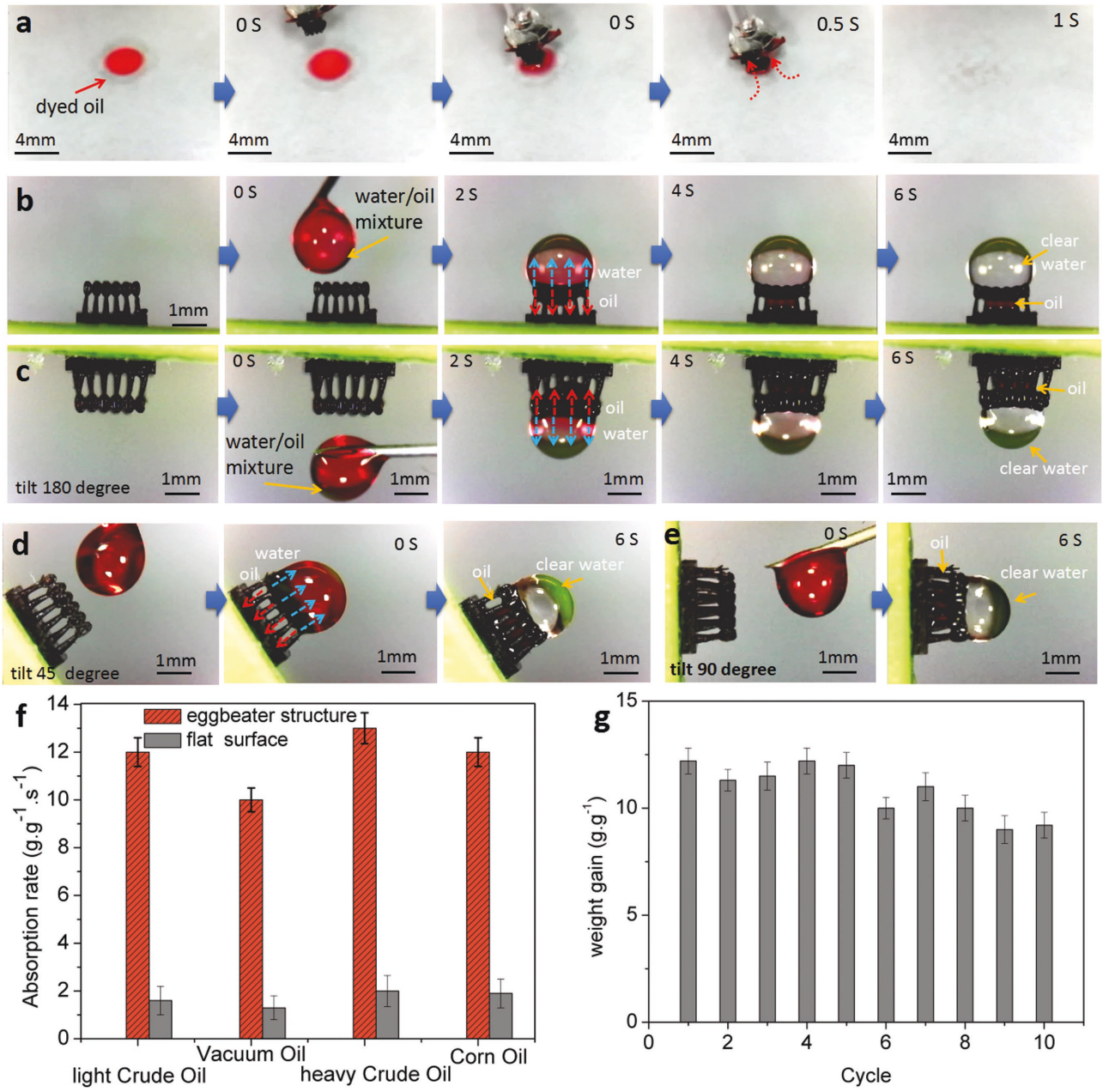


**Figure 5.** a) oil absorption of the 3D-printed eggbeater structures in 1 s (red arrows show the absorption of oil); oil/water mixture separation by the printed eggbeater structure in 6 s for horizontal eggbeater structure b), tilt upside down for 180° c) and tilt for 45° d) and 90° e), respectively; f) comparison of absorption rate for different types of oil; and g) changes of weight gain with different cycles.

with controllable adhesion. Furthermore, considering the efficient fabrication strategy of our method, the 3D-printed structures are potentially useful in biomedical and environmental engineering, such as microdroplet manipulation, droplet-based biodetection, drug test, and massive oil/water separation.

## Experimental Section

*Preparation of Polymer/MWCNTs Composite Resin*: The photocurable polymer resin E-glass was purchased from Envisiontec (Dearborn, MI) and used as received. MWCNTs (length (1–5 µm) and outer diameter (5–15 nm), from Bucky USA Inc.) was mixed with polymer resin for 2 h under a magnetic stirring and then ultrasonic bath for 30 min. The composite was degassed in the vacuum before fabrication. Oil red dye was purchased from Sigma Aldrich. Light and heavy crude oils were purchased from ONTA. Premium Quality Mechanical Vacuum oil was purchased from Edwards (Ultragrade 19). Kroger food colors (blue, red, yellow) were purchased from Amazon to make the dyed water. The super-hydrophobic and oleophobic nanocoating was purchased from Ultra-Ever Dry.

*Immersed Surface Accumulation System Design*: Inspired by the multi-axis CNC accumulation process, the immersed surface accumulation system consisted of an optical system, a mechanical system, and a light guide tool changing system.[68] Visible light source was used in the

optical system. To minimize the chromatic aberration, a fluorescence imaging filter (purchased from Throlabs, Inc.) was added to block most of lights that had wavelengths other than 405 nm. By controlling the angle of the micromirrors, the DMD chip could individually set the brightness of each pixel in the light beam. Except that, an achromatic doublet lens with focus $f_{ad}$ = 150 mm (purchased from Throlabs Inc.) was used to converge the light beams reflected by DMD chip. The collimated light went through the light guide tool which was mounted 4× Olympus plan achromatic objective lens with focus distance $f$ = 15 mm (purchased from Throlabs Inc.). The objective lens determined the desired dimension of the 2D light beam. The distance between the objective lens and the collimated lens can be changed based on the optical design (see Figure 2b). Multi-axis movements were integrated to change the angle of the inserted object so that features could be deposited from different surface orientations. Motivated by an automatic tool changing system in the traditional CNC machining system, a similar light guide tool changing system was developed to address the problem of building features on different object surfaces. In addition, a bottom-up frame was designed so that less resin could be used in the fabrication of microscale features (see Figure 2a).

*ISA-3D Printing of Micro Eggbeater Structure*: Optimizing the super-hydrophobic performance of micro eggbeater structures requires precise control over their shape and size. The eggbeater structure array model was firstly created using Solidworks (Figure 3a) and then sliced by an in-house developed "DMD-based SL" software to get different 2D patterns (Figure S1k, Supporting Information). For the generation of light beam with complex 2D microscale patterns, it needs to be correctly focused. A vision system containing a beam splitter, a convex lens and a CMOS camera was designed in the setup to observe the light beam for focusing adjustment. The captured image was displayed on a computer monitor with 50× magnifications (Figure 2d). Based on it, the focusing accuracy of the accumulation image can be adjusted. To make sure the following cured layers to stick onto the previously built layers, the moving speed of light guide tool was controlled to be 10–150 µm $s^{-1}$, which was determined by the light intensity and the cure depth of the photocurable resin.[68] At the same time, the exposure time was set based on the previous study and the fabrication data. The eggbeater structures form the overhang feature as shown in Figure 3a. The cure-depth of material used in this study was controlled to be 35 µm under full exposure by adding 0.5 wt% MWCNTs to avoid over cure in the fabrication direction.[68]

*Calculation of the Adhesion Force for the Eggbeater Structure with Different Number of Arms*: The principle of the capillary adhesion technique is shown in Figure S7 in the Supporting Information, in which a single eggbeater structure was fixed at its base with a reverse action tweezer. The tweezer was fixed on a stepper motor with the eggbeater tip facing downward. Then the tip was brought into contact with the surface of water. When the printed eggbeater structure was pulled upward, a meniscus was developed, which was eventually released when its tensile force exceeded the water adhesion force on the tip. A constant pulling velocity of 2 mm $min^{-1}$ was used. The whole pulling process was captured with a microscope, allowing the monitoring of both the meniscus shape and the deformation of the structure (the calculation process is discussed in the Supporting information). For each number of $N$, five different eggbeater shaped structures were examined to study the adhesive force.

*Test of Super-Hydrophobic Property*: For the test of super-hydrophobic property, a water droplet was placed on the top by a syringe needle. The droplet keeps a round shape for $N > 2$ and merges into the structure for $N = 0$. The picture of the formed droplet was taken by an optical microscope from the side view and was then inserted into an "Image J Software."[69] The contact angle was calculated by the Software for different number of arms and gaps.

*Oil/Water Separation*: To observe the oil absorption process, a glass tank containing water was placed on a table and oil droplets were added. The oil droplets will form a round shape on the surface due to the low density and surface tension. An optical microscope was placed to monitor the oil absorption process. Several different kinds of oil (light and heavy crude oil, vacuum oil, corn oil) were added separately. To calculate the absorption rate, the weight of the printed eggbeater structure and the absorbed oil was tested by OHAUS Adventurer Analytical Balance separately. The absorption time was observed from the test video. For the test of oil/water separation, eggbeater structures with different number of arms were firstly fabricated. Then an oil/water mixture droplet was placed onto the top of the eggbeater structure using a syringe. The separation process was captured with an optical microscope in the side view. In order to clearly observe the separation process, oil was dyed using Oil Red Dye purchased from Sigma-Aldrich. 0.1 g Oil Red Dye was added into 5 mL oil and using the magnetic stirrer for 10 min followed by ultrasonic for 5 min to promote the dissolve and homogeneous distribution. In order to test the flexibility of the 3D-printed eggbeater structure, the array was tilted for 45°, 90°, and 180°, respectively. The whole separation process was also observed by an optical microscope from the side view.

## Supporting Information

Supporting Information is available from the Wiley Online Library or from the author.

## Acknowledgements

Y.Y. and X.L. contributed equally to this work. The authors acknowledge the support from National Science Foundation (NSF) (Grant Nos. CMMI 1335476, CMMI-1151191, and CMMI 1663663) and USC's Epstein Institute. The authors also thank Prof. Keyue Shen and Hoang Peter Ta for their help with the 3D cancer cell culture. Thanks to the Center for Electron Microscopy and Microanalysis at USC for the SEM images measurement, and Prof. Steven Nutt and Daniel Zebrine for their help with the thermogravimetric analysis.

## Conflict of Interest

The authors declare no conflict of interest.

## Keywords

3D printing, biomimetic structures, droplet manipulation, oil/water separation, super-hydrophobic structures

Received: August 27, 2017
Revised: October 24, 2017
Published online:

[1] X. Gao, L. Jiang, *Nature* **2004**, *432*, 36.
[2] K. Autumn, Y. A. Liang, S. T. Hsieh, W. Zesch, W. P. Chan, T. W. Kenny, R. Fearing, R. J. Full, *Nature* **2000**, *405*, 681.
[3] B. Bhushan, *Philos. Trans. R. Soc. A* **2009**, *367*, 1445.
[4] K. Koch, B. Bhushan, W. Barthlott, *Prog. Mater. Sci.* **2009**, *54*, 137.
[5] X. Yao, Y. Song, L. Jiang, *Adv. Mater.* **2011**, *23*, 719.
[6] R. Blossey, *Nat. Mater.* **2003**, *2*, 301.
[7] A. Lafuma, D. Quéré, *Nat. Mater.* **2003**, *2*, 457.
[8] M. J. Hancock, K. Sekeroglu, M. C. Demirel, *Adv. Funct. Mater.* **2012**, *22*, 2223.
[9] Y. Zhu, J. Zhang, Y. Zheng, Z. Huang, L. Feng, L. Jiang, *Adv. Funct. Mater.* **2006**, *16*, 568.
[10] J. Yuan, X. Liu, O. Akbulut, J. Hu, S. L. Suib, J. Kong, F. Stellacci, *Nat. Nanotechnol.* **2008**, *3*, 332.

 

[11] M. Jin, J. Wang, X. Yao, M. Liao, Y. Zhao, L. Jiang, *Adv. Mater.* **2011**, *23*, 2861.
[12] Z. Xue, S. Wang, L. Lin, L. Chen, M. Liu, L. Feng, L. Jiang, *Adv. Mater.* **2011**, *23*, 4270.
[13] W. L. Min, B. Jiang, P. Jiang, *Adv. Mater.* **2008**, *20*, 3914.
[14] M. Jin, X. Feng, L. Feng, T. Sun, J. Zhai, T. Li, L. Jiang, *Adv. Mater.* **2005**, *1*, 1977.
[15] X. J. Feng, L. Jiang, *Adv. Mater.* **2006**, *18*, 3063.
[16] D. Quéré, *Nat. Mater.* **2002**, *1*, 14.
[17] W. Barthlott, T. Schimmel, S. Wiersch, K. Koch, M. Brede, M. Barczewski, S. Walheim, A. Weis, A. Kaltenmaier, A. Leder, H. F. Bohn, *Adv. Mater.* **2010**, *22*, 2325.
[18] A. Solga, Z. Cerman, B.F. Striffler, M. Spaeth, W. Barthlott, *Bioinspiration Biomimetics* **2007**, *2*, S126.
[19] O. Tricinci, T. Terencio, B. Mazzolai, N. M. Pugno, F. Greco, V. Mattoli, *ACS Appl. Mater. Interfaces* **2015**, *7*, 25560.
[20] N. Zhao, Q. Xie, X. Kuang, S. Wang, Y. Li, X. Lu, S. Tan, J. Shen, X. Zhang, Y. Zhang, J. Xu, C. C. Han, *Adv. Funct. Mater.* **2007**, *17*, 2739.
[21] Y. Lai, X. Gao, H. Zhuang, J. Huang, C. Lin, L. Jiang, *Adv. Mater.* **2009**, *21*, 3799.
[22] F.D. Nicola, P. Castrucci, M. Scarselli, F. Nanni, I. Cacciotti, M.D. Crescenzi, *Nanotechnology* **2015**, *26*, 145701.
[23] Y. Yang, Z. Chen, X. Song, B. Zhu, T. Hsiai, P.I. Wu, R. Xiong, J. Shi, Y. Chen, Q. Zhou, K.K. Shung, *Nano Energy* **2016**, *22*, 414.
[24] W. Gao, Y. Zhang, D. Ramanujan, K. Ramani, Y. Chen, C. B. Williams, C. C. L. Wang, Y. C. Shin, S. Zhang, P.D. Zavattieri, *Comput. Aided Des.* **2015**, *69*, 65.
[25] J. Zou, H. Chen, A. Chunder, Y. Yu, Q. Huo, L. Zhai, *Adv. Mater.* **2008**, *20*, 3337.
[26] J. E. Mates, I. S. Bayer, J. M. Palumbo, P. J. Carroll, C. M. Megaridis, *Nat. Commun.* **2015**, *6*, 8874.
[27] R. N. Wenzel, *Ind. Eng. Chem.* **1936**, *28*, 988.
[28] J. Friedrich, C. Seidel, R. Ebner, L. A. Kunz-Schughart, *Nat. Protoc.* **2009**, *4*, 309.
[29] S. Lee, B. Kim, S. H. Kim, E. Kim, J.H. Jang, *Adv. Funct. Mater.* **2017**, *27*, 1702310.
[30] L. Feng, S. Li, Y. Li, H. Li, L. Zhang, J. Zhai, Y. Song, B. Liu, L. Jiang, D. Zhu, *Adv. Mater.* **2002**, *14*, 1857.
[31] B. Bhushan, E. K. Her, *Langmuir* **2010**, *26*, 8207.
[32] J. Yuan, X. Liu, O. Akbulut, J. Hu, S. L. Suib, J. Kong, F. Stellacci, *Nat. Nanotechnol.* **2008**, *3*, 332.
[33] X. Hong, X. F. Gao, L. Jiang, *J. Am. Chem. Soc.* **2007**, *129*, 1478.
[34] D. Quéré, *Annu. Rev. Mater. Res.* **2008**, *38*, 71.
[35] Z. Cheng, M. Du, H. Lai, N. Zhang, K. Sun, *Nanoscale* **2013**, *5*, 2776.
[36] X. Tang, P. Zhu, Y. Tian, X. Zhou, T. Kong, L. Wang, *Nat. Commun.* **2017**, *8*, 14831.
[37] J. Lv, Z. Gong, Z. He, J. Yang, Y. Chen, C. Tang, Y. Liu, M. Fan, W. M. Lau, *J. Mater. Chem. A* **2017**, *5*, 12435.
[38] Y. Chen, C. Zhou, J. Lao, *Rapid Prototyping J.* **2011**, *17*, 218.
[39] X. Zhao, Y. Pan, C. Zhou, Y. Chen, C. C. L. Wang, *J. Manuf. Processes* **2013**, *15*, 432.
[40] H. Mao, C. Zhou, Y. Chen, *J. Manuf. Processes* **2016**, *24*, 406.
[41] Y. Pan, C. Zhou, Y. Chen, J. Partanen, *ASME J. Manuf. Sci. Eng.* **2014**, 136.
[42] G. Whyman, E. Bormashenko, T. Stein, *Chem. Phys. Lett.* **2008**, *450*, 355.
[43] D. Gandyra, S. Walheim, S. Gorb, W. Barthlott, T. Schimmel, *Beilstein J. Nanotechnol.* **2015**,*6*, 11.
[44] A. J. DeMello, *Nature* **2006**, *442*, 394.
[45] B. Su, S. Wang, Y. Song, L. Jiang, *Soft Matter* **2012**, *8*, 631.
[46] H. Song, D. L. Chen, R. F. Ismagilov, *Angew. Chem., Int. Ed.* **2006**, *45*, 7336.
[47] W. S. Y. Wong, P. Gutruf, S. Sriram, M. Bhaskaran, Z. Wang, A. Tricoli, *Adv. Funct. Mater.* **2016**, *26*, 399.
[48] Y. Lai, F. Pan, C. Xu, H. Fuchs, L. Chi, *Adv. Mater.* **2013**, *25*, 1682.
[49] L. Yu, M. C. W. Chen, K. C. Cheung, *Lab Chip.* **2010**, *10*, 2424.
[50] I. Amjadi, M. Rabiee, M. S. Hosseini, M. Mozafari, *Appl. Biochem. Biotechnol.* **2012**, *168*, 1434.
[51] K. Li, J. Ju, Z. Xue, J. Ma, L. Feng, S. Gao, L. Jiang, *Nat. Commun.* **2013**, *4*, 2276.
[52] M.A. Shannon, P.W. Bohn, M. Elimelech, J. G. Georgiadis, B.J. Marinas, A.M. Mayes, *Nature* **2008**, *452*, 301.
[53] Y. Zhao, M. Zhang, Z. Wang, *Adv. Mater. Interfaces* **2016**, *3*, 1500664.
[54] A. Soudmand-Asli, S. S. Ayatollahi, H. Mohabatkar, M. Zareie, S. F. Shariatpanahi, *J. Pet. Sci. Eng.* **2007**, *58*, 161.
[55] W. Choi, A. Tuteja, S. Chhatre, J. M. Mabry, R. E. Cohen, G. H. McKinley, *Adv. Mater.* **2009**, *21*, 2190.
[56] A. B. Koltuniewicz, R. W. Field, T. C. Arnot, *J. Membr. Sci.* **1995**, *102*, 193.
[57] X. Zheng, Z. Guo, D. Tian, X. Zhang, L. Jiang, *Adv. Mater. Interfaces* **2016**, *3*, 1600461.
[58] G. Kwon, A. K. Kota, Y. Li, A. Sohani, J. M. Mabry, A. Tuteja, *Adv. Mater.* **2012**, *24*, 3666.
[59] C. Zeiger, I. C. R. da Silva, M. Mail, M. N. Kavalenka, W. Barthlott, H. Hölscher, *Bioinspiration Biomimetics* **2016**, *11*, 056003.
[60] Z. Xue, M. Liu, L. Jiang, *J. Polym. Sci., Part B: Polym. Phys.* **2012**, *50*, 1209.
[61] A. K. Kota, G. Kwon, W. Choi, J. M. Mabry, A. Tuteja, *Nat. Commun.* **2012**, *3*, 1025.
[62] T. Ichikawa, K. Itoh, S. Yamamoto, M. Sumita, *Colloids Surf., A* **2004**, *242*, 21.
[63] H. Sun, Z. Xu, C. Gao, *Adv. Mater.* **2013**, *25*, 2554.
[64] X. Gui, J. Wei, K. Wang, A. Cao, H. Zhu, Y. Jia, Q. Shu, D. Wu, *Adv. Mater.* **2010**, *22*, 617.
[65] H. Bi, X. Xie, K. Yin, Y. Zhou, S. Wan, L. He, F. Xu, F. Banhart, L. Sun, R. S. Ruoff, *Adv. Funct. Mater.* **2012**, *22*, 4421.
[66] J. Song, Y. Lu, J. Luo, S. Huang, L. Wang, W. Xu, I. P. Parkin, *Adv. Mater. Interfaces* **2015**, *2*, 1500350.
[67] P. Calcagnile, D. Fragouli, I. S. Bayer, G. C. Anyfantis, L. Martiradonna, P. D. Cozzoli, R. Cingolani, A. Athanassiou, *ACS Nano* **2012**, *6*, 5413.
[68] X. Li, Y. Chen, *J. Manuf. Processes* **2017**, *28*, 531.
[69] A. F. Staldera, T. Melchiorb, M. Müllerb, D. Saged, T. Blu, M. Unser, *Colloid Surf. A: Physicochem. Eng. Asp.* **2010**, *364*, 72.